ChemPubSoc Europe

DOI: 10.1002/cctc.201500606

CHEMCATCHEM Communications

Design of Artificial Metabolisms in Layered Nanomaterials for the Enzymatic Synthesis of Phosphorylated Sugars

Rima Mahdi,[a, b] Christine Guérard-Hélaine,[a, b] Vanessa Prévot,[a, b] Véronique de Berardinis,[c, d, e] Claude Forano,*[a, b] and Marielle Lemaire*[a, b]

This manuscript is dedicated to Wolf-Dieter "Woody" Fessner on the occasion of his 60th birthday.

Biohybrid nanoreactors operating in one-pot cascade reactions were designed by co-immobilization of enzymes in an inorganic layered matrix, namely, layered double hydroxides. These biohybrid systems were devoted to prepare dihydroxyacetone phosphate (DHAP) and phosphorylated sugars through stereoselective C–C bond formation. In the first system, two kinases were exploited for the in situ generation of DHAP. Increasing the complexity, the second nano-bioreactor combined up to four enzymes to lead to D-fructose-6-phosphate from the aldol-catalyzed addition of dihydroxyacetone to D-glyceraldehyde-3-phosphate generated in situ from DHAP. The biohybrid catalyst showed the same reaction rate as that of the free enzymes and was reusable.

Tandem and cascade reactions were highlighted by Trost et al. in 2008[1] as being of fundamental importance to develop greener syntheses. Biocatalysis takes a major place in this field, in particular enzymatic cascades, which create artificial pathways for the preparation of chiral or complex chemicals.[2] This emerging concept was recently termed "system biocatalysis" by Fessner.[3] Nature can be mimicked by designing artificial metabolic and non-natural biocatalytic pathways in vitro. In such multienzymatic systems, enzymes are brought together in the same reaction vessel, in which the product of one enzyme is the substrate of the other. The reaction parameters (e.g., pH, enzyme quantity, substrate concentration, cosolvent, temperature, etc.) are easier to control than in in vivo systems and can be adjusted to reach high yields and purities.[4–6] To approach natural systems for which the cooperating enzymes are organized in specific assemblies leading, in some cases, to a channeling effect, the artificial metabolic pathways can be immobilized following different strategies. They have been nicely reviewed by Schoffelen et al.[5] The strategies are classified in order of increasing control of the enzyme organization: random co-immobilization to a solid support (e.g., agarose,[7] chitin,[8] nylon,[8] polystyrene,[9] polyvinyl chloride[10]) or nanoparticles (e.g., gold nanoparticles,[11] sol–gel matrix[12]), sequential immobilization in microfluidic channels, positional immobilization on DNA nanostructures, site-specific enzyme immobilization, and finally scaffold-free cross-linking.

In this work, we aim to design cascade reactions for the enzymatic synthesis of phosphorylated sugars following the random co-immobilization of enzymes embedded in layered double hydroxide (LDH) nanoplatelets. Indeed LDHs, $M^{II}_{1-x}M^{III}_{x}(OH)_2X_{x/q}\cdot n\,H_2O$ (Supporting Information, Scheme S1), owing to their two-dimensional structure, physicochemical properties, and controllable nanoplatelet aggregation,[13] offer a suitable microenvironment that favors a high loading of enzymes, an increase in their stability, and preservation of their activity.[14] In the course of our work on green by design, efficient cascades for the enzymatic synthesis of terminally phosphorylated sugars as key metabolites were implemented. They were based on the in situ formation of chiral or achiral synthons[15,16] such as, for example, D-glyceraldehyde-3-phosphate (D-G3P) from dihydroxyacetone phosphate (DHAP)[17] (Scheme S2). The key enzymes fructose-6-phosphate aldolase wildtype (FSA_{wt}) from *Escherichia coli* and its variant (i.e., FSA_{A129S}) were involved in stereoselective C–C bond formation. The wild-type aldolase was efficiently immobilized in LDH,[18] and more recently, a bioreactor was elaborated by hierarchical assembly of FSA_{wt}, LDH nanoplatelets, and polysaccharide.[19] To build a complex cascade system and to reach the concept of an immobilized artificial metabolism, four different enzymes, two kinases [i.e., dihydroxyacetone kinase (DHAK) and pyruvate kinase PK_{Gstea}], a triosephosphate isomerase (TPI), and fructose-6-phosphate aldolase (FSA_{A129S}) were immobilized. Such a LDH-based biohybrid was evaluated in particular to produce D-fructose-6-phosphate (D-F6P) by using dihydroxyacetone (DHA) as a donor substrate for the aldolase (Scheme 1). In addition, DHAP production will be studied inde-

[a] R. Mahdi, Dr. C. Guérard-Hélaine, Dr. V. Prévot, Prof. C. Forano, Prof. M. Lemaire
Institut de Chimie de Clermont-Ferrand
Université Clermont Auvergne, Université Blaise Pascal
BP 10448, F-63000 Clermont-Ferrand (France)
E-mail: marielle.lemaire@univ-bpclermont.fr
claude.forano@univ-bpclermont.fr

[b] R. Mahdi, Dr. C. Guérard-Hélaine, Dr. V. Prévot, Prof. C. Forano, Prof. M. Lemaire
CNRS, UMR 6296, ICCF
F-63177 Aubière (France)

[c] Dr. V. de Berardinis
CEA, DSV, IG, Genoscope
BP 91057 Evry (France)

[d] Dr. V. de Berardinis
CNRS, UMR 8030
91057 Evry (France)

[e] Dr. V. de Berardinis
Université d'Evry Val d'Essonne
BP 91057 Evry (France)

Supporting Information for this article is available on the WWW under http://dx.doi.org/10.1002/cctc.201500606.

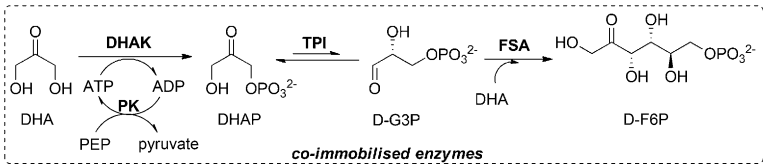

Scheme 1. Synthesis of D-F6P from DHA by using a four-enzyme bio-nanoreactor. AD(T)P = adenosine di(tri)phosphate; PEP = phosphoenolpyruvate.

pendently by the immobilization of two kinases and used with non-immobilized aldolases.

To promote enzyme co-immobilization, a direct LDH co-precipitation strategy was systematically followed consisting of metal salt precipitation in the presence of enzymes at an appropriate pH and under soft conditions (e.g., room temperature, water). Given that the physicochemical surface properties (e.g., charge density, acido-basicity) of LDHs strongly depend on the layer metal cations that impact the enzyme adsorption and activity,[20] three different compositions of the LDHs were considered: Mg_2Al-LDH, Zn_2Al-LDH, and MgZnAl-LDH. The four enzymes involved in the process were DHAK[21] (E.C. 2.7.1.29 from *Citrobacter freundii*), PK_{Gstea} (E.C. 2.7.1.40 from *Geobacillus stearothermophilus*), TPI (E.C. 5.3.1.1 from *Saccharomyces cerevisiae*), and the variant FSA_{A129S}[22] (E.C. 4.1.2 from *E. coli*). The enzyme/LDH ratios were fixed according to the specific activities of the enzymes and the results described for the non-immobilized system involved to prepare D-F6P.[17] The results obtained for the four enzymes are gathered in Table 1.

Preliminarily, two commercially available PK from rabbit muscle and from *G. stearothermophilus* (PK_{Gstea}) were tested, and it was revealed that PK_{Gstea} was the more stable enzyme, as 90% activity loss of PK from rabbit muscle was observed after immobilization. Owing to its high cost, the chosen PK_{Gstea} (Unitprot ID Q02499) was thus cloned, overexpressed in *E. coli* as N-terminal histidine (His)-tagged recombinant protein, and purified (see the Supporting Information). TPI was used as a commercial preparation, and DHAK and FSA_{A129S} were prepared as previously described.[21,22]

For the whole set of enzymes, the same conditions as those previously reported for FSA_{wt} immobilization were applied.[18]

Table 1. Results of immobilization of PK_{Gstea}, DHAK, TPI, and FSA_{A129S}.

Enzyme	Matrix	LDH/enzyme	Encapsulation efficiency [%]	Retained activity/immobilized theoretical activity [U]	Retained activity [%]
PK_{Gstea}	Mg_2Al	1:0.14	100	158/353	45 ± 5
	Zn_2Al	1:0.14	100	187/369	51 ± 5
	MgZnAl	1:0.14	100	194/360	54 ± 5
DHAK	Mg_2Al	1:1	100	9.5/21	45 ± 5
	Zn_2Al	1:1	100	9/20	45 ± 5
	MgZnAl	1:1	100	10/20	50 ± 5
TPI	Mg_2Al	1:0.005	100	540/1495	36 ± 5
	Zn_2Al	1:0.005	100	1342/1470	90 ± 5
	MgZnAl	1:0.005	100	1281/1480	87 ± 5
FSA_{A129S}	Mg_2Al	1:1	100	183/200	92 ± 5
	Zn_2Al	1:1	50	302/418	72 ± 5
	MgZnAl	1:1	100	70/80	88 ± 5

Up to 100% of the protein quantities (Bradford assay) were immobilized in the Mg_2Al, Zn_2Al, and MgZnAl LDH matrices, except in the case of FSA_{A129S} in Zn_2Al (50%). This demonstrates the exceptional ability of the LDH materials to encapsulate a large variety of enzymes in their structure. Unlike TPI, the most suitable LDH matrices were those containing Mg, for which FSA_{A129S} was totally immobilized with 90% retained activity. The Zn-based matrix gave lower immobilization rates with only 50% trapped protein but the activity was acceptably maintained at 72%. In this latter case, by taking into account the high loading of the enzyme (1:1), this selectivity may be explained by the surface charge of the enzyme relative to that of LDH, as the isoelectric point [iep(FSA_{A129S})] and pH_{pzc}(LDH) have almost identical values; the lower the value of Δ[iep(enzyme) − pHp_{zc}(LDH)] (Table S1), the lower the electrostatic interactions and the enzyme loading.

None of these enzymes were previously immobilized in inorganic matrix, and these results open the field for elaboration of a novel generation of biohybrid supported catalysts.

To comment on the retention of enzymatic activity, the LDH host structures offer a suitable microenvironment for the preservation of the biocatalytic performances. Indeed, between 36 and 92% of the activity of the free enzyme was kept. However, the chemical composition of the LDH matrix has a noticeable effect on the catalytic activity of the immobilized enzymes. Interestingly, with some enzymes, tuning the metal cation composition allows the amount of retained activity to be improved (Table 1). For both kinases (i.e., PK_{Gstea} and DHAK), a decrease in the activity by 50% was observed after immobilization, regardless of the M^{II} composition (Table 1, entries 1 and 2). If TPI was immobilized in Mg_2Al, the retained activity was only 36%. Interestingly, if Mg was diluted into the three metal cation layer MgZnAl a higher value of retained activity was measured (87%). Even better, very good results were obtained for immobilized TPI within the Zn-based LDH matrix with quantitative immobilization of the protein and a retained activity of 90% (Table 1, entry 3). Note that as a result of the very high specific activity of TPI ($\approx$10000 U mg^{-1}), a very low amount of this enzyme was used for immobilization onto the LDH matrix (LDH/TPI = 1:0.005).

The storage stability at 4 °C of the different biohybrids (colloidal suspension) was investigated and compared to the stability of the free enzymes (Figure 1, see also Figure S1). Concerning FSA_{A129S}, TPI, and PK_{Gstea}, enhanced enzyme stability was observed once immobilized within LDH. The stabilizing effect is particularly highlighted. The most interesting results were obtained for immobilized PK_{Gstea}, which retained 95% of its activity after 1 month of storage, whereas free PK_{Gstea} lost 50% of its activity within the same timeframe. However, DHAK is a noteworthy exception because DHAK immobilization in LDH causes

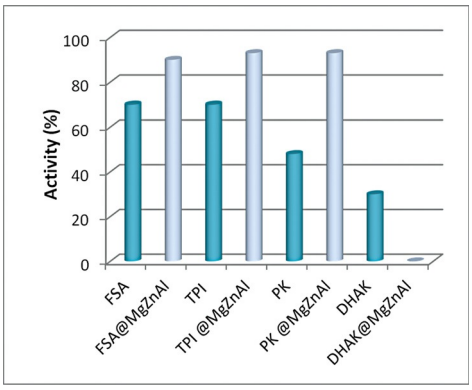

Figure 1. Storage stability at 4 °C of free enzymes (dark) and biohybrids (light) after 30 d except for DHAK (4 d). The conditions of storage for each enzyme were water, pH 7.5 for FSA_{A129S}; Tris buffer (15 mM), pH 7.5 for TPI; Tris buffer (15 mM), $MgCl_2$ (5 mM), KCl (5 mM), pH 7.5 for PK_{Gstea}; and Tris buffer (15 mM), $MgCl_2$ (5 mM), pH 7.5 for DHAK.

an increase in enzyme instability relative to that of the free enzyme (Figure S1). Free or immobilized, DHAK is unstable, and its instability increases upon immobilization. This instability could be due to the His tag or/and a negative allosteric effect of the Mg cation, as discussed recently by Wang et al.[23]

The activity was completely lost after 4 days, whereas the free enzyme retained 40% of its activity. To circumvent this disadvantage, we are looking for a more stable DHAK with a different His tag construction or found in the biodiversity.

The nanostructures of the enzyme@LDH biohybrid materials were investigated by powder X-ray diffraction and FTIR spectroscopy (see the Supporting Information). The diffractograms of the different biohybrids (Figure 2, see also Figure S2) show typically amorphous structures as a result of the preferential structuration of the LDH nanoplatelets around the enzyme, which act as nucleation promoters. However, it should be noted that the systematic presence of the (012) and (110) diffraction lines and the typical LDH lattice vibration bands, M–OH, M–O, and O–M–O at $\tilde{\nu}=844$, 668, and 446 cm^{-1}, respectively, confirm the formation of the LDH hexagonal layer structure (i.e., space group $R\bar{3}m$). As previously reported,[24] the layer stacking (or crystal growth in the *c* direction) is strongly limited by surface adsorption of the enzyme, as evidenced by the almost total absence of any 00L diffraction lines, whereas the enzyme-free LDH phase prepared under the same conditions displays the 001 and 002 peaks characteristic of a 0.88 nm basal spacing. The amorphization of the layered structure caused by the presence of an enzyme was also confirmed by enlargement of the lattice vibration bands of the biohybrid materials relative to the bands of the nitrate-intercalated LDH reference materials.

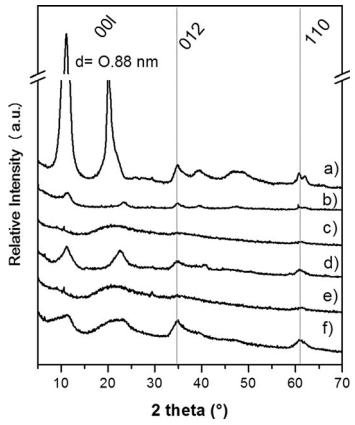

Figure 2. PXRD patterns of a) MgAlZn–NO_3 LDH, and MgAlZn prepared in the presence of b) TPI, c) DHAK, d) PK_{Gstea}, e) FSA_{A129S}, and f) the four enzymes TPI, DHAK, PK_{Gstea}, and FSA_{A129S}.

Enzyme immobilization was further evidenced for all biohybrids by FTIR spectroscopy (vibration bands of the amide group at $\tilde{\nu}=1660$ and 1540 cm^{-1} and the CH bond at $\tilde{\nu}=$ 2960 cm^{-1}). Notably, the decrease in the intensity of the $-NO_3$ valence band ($\tilde{\nu}=1368$ cm^{-1}) evidences partial anion exchange by the enzymes (Figure S3).

In the first part of this work, the two kinase enzymes were conjointly immobilized in a LDH bio-nanoreactor to produce DHAP from DHA by using DHAK; the pyruvate kinase/phosphoenolpyruvate (PK_{Gstea}/PEP) system allowed regeneration of the required ATP cofactor (Scheme 1).

To determine the efficiency of the biohybrids, DHAP synthesis was performed and compared to the same synthesis with the free enzyme by keeping the number of units of each enzyme constant (see the Supporting Information). The rate of DHAP formation by using co-immobilized enzymes (Figure 3, see also Figure S4a,b) was the same as that with the free enzymes. To determine the recyclability of the system, three cycles were performed with the biohybrid (Figure S4c,d). A high level of enzyme activity was kept over a few biocatalysis reaction cycles. Only after the third cycle did the PK_{Gstea} and DHAK activities fall to 75 and 30%, respectively, but the formation of DHAP was still ensured (Table S2). For the first time, two kinases were co-immobilized and used to produce a highly valuable phosphorylated synthon.

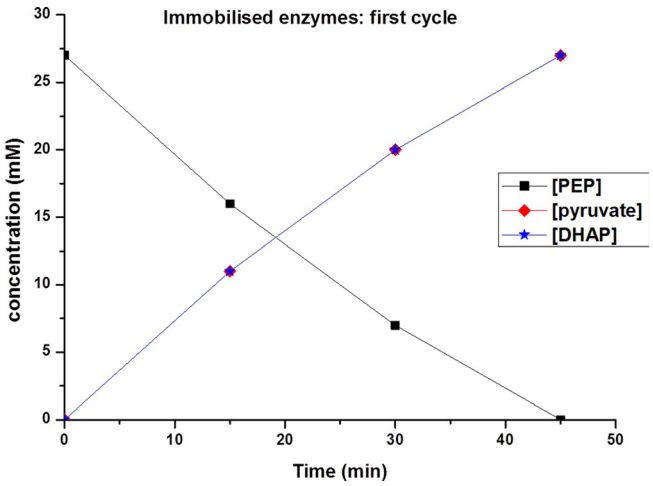

Figure 3. Rate of DHAP formation by using the PK_{Gstea}–DHAK@Mg_2Al nanobioreactor. Conditions: DHA (0.4 mmol), PEP (0.64 mmol), ATP (52 μmol), $MgCl_2$ (10 mM); pH adjusted to 7.5; DHAK (20 U) and PK_{Gstea} (20 U). Concentrations of PEP, pyruvate, and DHAP were followed by using a spectrophotometric assay.

Given that DHAP is a key substrate for DHAP-dependent aldolases to prepare various 1-phosphorylated sugars,[17,25,26] the efficiency of the PK_{Gstea}–DHAK@Mg_2Al biohybrid was evaluated for four reactions by using commercially available rabbit muscle aldolase (RAMA, 3*S*,4*R* stereoselective) and rhamnulose aldolase (RhuA, 3*R*,4*S* stereoselective) produced and purified as already described.[27] These aldolases were used with two acceptors, glycolaldehyde and D-glyceraldehyde (Scheme 2, see also Scheme S3). The three matrices give similar results with the two kinases (encapsulation efficiency of 100% and immobilized activities of 50%; Table 1), and to limit DHAP isomerization into D-G3P, the co-immobilization was preferentially conducted in Mg_2Al–LDH to minimize TPI activity (36% of retained activity, see Table 1), often present as a contaminant enzyme. Indeed, TPI can afford D-G3P, which can react with DHAP in the presence of RAMA to produce D-fructose-1,6-bisphosphate as a byproduct. Under these conditions, RAMA provides D-xylulose-1-phosphate[28] and D-fructose-1-phosphate,[29] whereas RhuA leads to L-xylulose-1-phosphate[28] and D-sorbose-1-phosphate.[30] To completely shift the equilibrium to sugar formation, 2 equivalents of acceptor aldehydes was added and no more DHAP was detected. All the products were successfully purified by barium precipitation (see the Supporting Information), and yields of 75, 80, 79, and 78% were obtained for L-xylulose-1-phosphate, D-fructose-1-phosphate, D-sorbose-1-phosphate, and D-xylulose-1-phosphate, respectively.

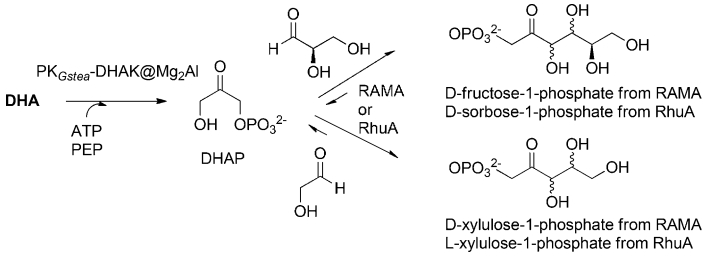

Scheme 2. Enzymatic cascade reactions with the PK_{Gstea}–DHAK@Mg_2Al biohybrid for the preparation of phosphorylated sugars.

Encouraged by these very good results, we decided to design, in the second part of the work, a four-enzyme bio-nanoreactor involving PK_{Gstea}, DHAK, TPI, and FSA_{A129S} to synthesize D-F6P as a model reaction (Scheme 1). This sequence was performed in a one-pot cascade reaction. First, DHAP is formed by phosphorylation of DHA by using ATP-dependent DHAK. Then, isomerization of DHAP into D-G3P occurs under catalysis of TPI.[17] Finally, aldolization between DHA and D-G3P by using FSA_{A129S} shifts the equilibrium (Scheme 1) to the formation of D-F6P.

According to the results obtained for the individual enzyme immobilizations, the MgZnAl-LDH matrix was selected to prepare such a biohybrid, as it displayed higher enzyme loading and retained higher enzyme activity. Direct coprecipitation was performed in a medium containing a determined quantity of each enzyme, following the previous results obtained for the free enzyme system[17] and taking into account the observed loss in activity in the LDH. Typically, 45 mg of DHAK (182 U), 2.5 mg of FSA_{A129S} (13 U), 1 mg of PK_{Gstea} (92 U), and 0.1 mg of TPI (1638 U) were used, corresponding to an enzyme/LDH ratios of 1:1, 1:20, 1:50, and 1:500 for DHAK, FSA_{A129S}, PK_{Gstea}, and TPI, respectively. Note that owing to its instability, a larger amount of DHAK was involved in the biohybrid. As a result, 100% of the proteins were immobilized, and the retained activities were in the same order of magnitude as those obtained if the individually immobilized enzymes were considered: 50, 50, 90, and 92% for DHAK, PK_{Gstea}, TPI, and FSA_{A129S}, respectively. As observed for single enzymes, the XRD pattern of the biohybrid traduced the formation of an ill-defined LDH structure (Figure 2 f), which confirmed for the first time the possibility to extend such a strategy to multi-enzymatic LDH preparation. The efficiency of this bio-nanoreactor was compared with that of the free enzymes. The rate of D-F6P formation was the same as that if the immobilized system or the free enzyme were used (see the Supporting Information). Owing to the high quantity of DHAK, DHA phosphorylation was faster than the aldolization, as indicated by the higher rate of pyruvate formation relative to that of D-F6P. The D-F6P generated by the biohybrid was purified and isolated in 90% yield, as confirmed by NMR spectroscopy (see the Supporting Information).

The biohybrid was reusable over three cycles (Figure 4, see also Figure S5). After each cycle, the activity of DHAK diminished as showed in Table 2, whereas the activities of FSA_{A129S}, PK_{Gstea}, and TPI remained stable at approximately 85% over the three cycles. As a consequence, this decreased activity of DHAK led to increased reaction times from 60 min for the second cycle to 70 min for the third one. In this latter case, the rates of formation of DHAP and D-F6P were the same, and consequently, the determinant step was probably the formation of

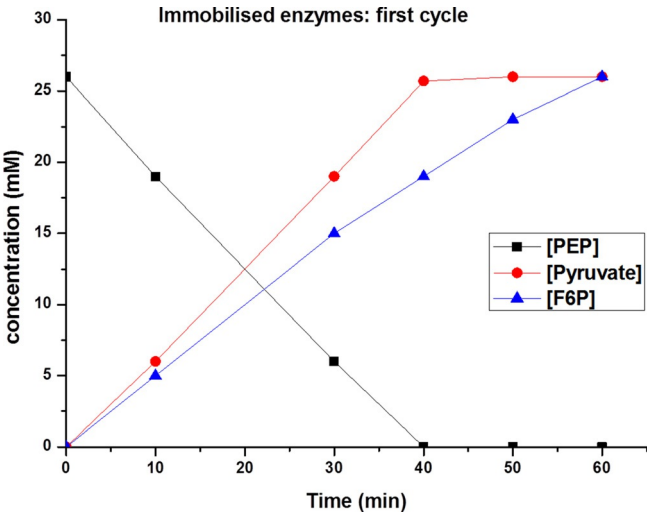

Figure 4. Rate of D-F6P formation by using the PK_{Gstea}–DHAK–TPI–FSA_{A129S}@MgZnAl biohybrid. Conditions: DHA (0.8 mmol, 2 equiv.), PEP (0.32 mmol), ATP (36 μmol), $MgCl_2$ (10 mM); pH adjusted to 7.5; DHAK (20 U), PK_{Gstea} (11 U), FSA_{A129S} (3 U), and TPI (288 U). The concentrations of pyruvate, D-F6P, and PEP were measured by spectrophotometric assays.

Table 2. Retained activities after each cycle for the PK_{Gstea}–DHAK–TPI–FSA_{A129S}@MgZnAl biohybrid.

Cycle	FSA_{A129S} activity [%]	PK_{Gstea} activity [%]	DHAK activity [%]	TPI activity [%]
1	96	95	60	97
2	88	90	36	90
3	84	86	22	85

DHAP. Finally, for the same quantity of D-F6P formed, the immobilized system allowed the use of 3-fold less U of FSA and TPI and 1.5-fold less U of DHAK and PK.

Concerning the stability of each enzyme in the bio-nanoreactor, it was observed that if the four-enzyme bio-nanoreactor was conserved in Tris buffer (15 mM), $MgCl_2$ (5 mM), and KCl (5 mM), the activity of DHAK was lost in 4 days, whereas the activities of PK_{Gstea}, FSA_{A129S}, and TPI remained unchanged for 1 month (Figure 5).

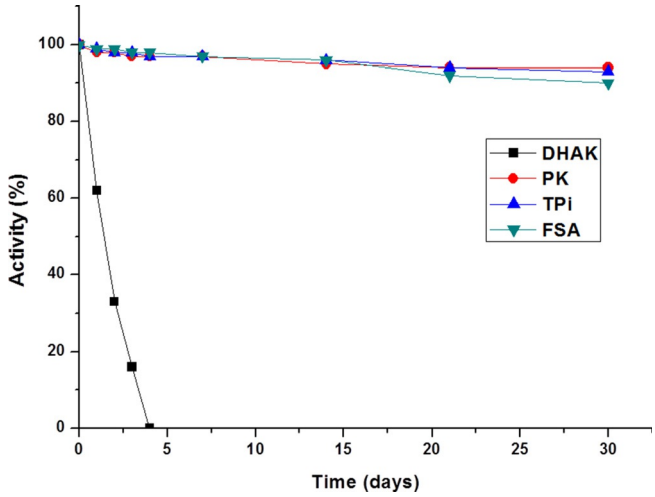

Figure 5. Storage stability of the four-enzyme biohybrid. The conditions of storage were Tris buffer (15 mM), $MgCl_2$ (5 mM), KCl (5 mM), pH 7.5.

In summary, we presented for the first time a study on multi-enzyme co-immobilization in layered double hydroxides (LDHs). A biohybrid system consisting of PK_{Gstea}—DHAK@Mg_2Al (PK_{Gstea} = pyruvate kinase, DHAK = dihydroxyacetone kinase) was first designed to synthesize dihydroxyacetone phosphate (DHAP). The same rate of DHAP formation was observed upon using the nano-biomaterial or the corresponding free enzymes; the biohybrid was reusable over three cycles. It was then employed to efficiently produce 1-phosphorylated sugars by adding a DHAP-dependent aldolase and an aldehyde acceptor to the reaction medium. Second, a four-enzyme system including an aldolase PK_{Gstea}–DHAK–TPI–FSA_{A129S}@MgZnAl (TPI = triosephosphate isomerase, FSA_{A129S} = fructose-6-phosphate aldolase) was designed to prepare D-fructose-6-phosphate (D-F6P) from dihydroxyacetone (DHA). The MgZnAl-LDH matrix showed 100% encapsulation efficiency and fair retained activities for the enzymes (≈50% for DHAK and PK_{Gstea}, 90% for FSA_{A129S} and TPI). D-F6P was obtained in 90% yield. This nano-biomaterial was reusable over three cycles and retained approximately 85% of the activities of PK_{Gstea}, FSA_{A129S}, and TPI and 22% of the activity of DHAK.

Experimental Section

Synthesis of DHAP

Co-immobilization of DHAK and PK_{Gstea} was realized as follows. Typically, a magnesium and aluminum nitrate salt solution (10.7 mL, $\Sigma[Mg^{2+} + Al^{3+}] = 0.1$ M, Mg/Al = 2:1) was added to a reactor containing DHAK (325 U, 90 mg) and PK_{Gstea} (295 U, 2.8 mg) dissolved in Tris buffer (50 mM, pH 9.0, 15 mL). With stirring and under a nitrogen atmosphere, the pH was kept at 9.0 during the immobilization process, which was complete in 200 min. The precipitate was washed by three dispersion/centrifugation cycles with deionized water. The biohybrid (160 mg) was obtained with 0.97 U DHAK (mg biohybrid)$^{-1}$ and 0.93 U PK_{Gstea} (mg biohybrid)$^{-1}$. The yield of the coprecipitation was 80%. The encapsulation efficiency was 100%, and the retained activities were 50% for DHAK and 48% for PK_{Gstea}. The biohybrid was conserved as a colloidal suspension in deionized water at 4 °C.

The synthesis of DHAP by using free or immobilized enzymes was realized as described previously with minor modifications.[17] DHA (0.4 mmol), phosphoenolpyruvate (PEP, 0.32 mmol), ATP (52 μmol), and $MgCl_2$ (10 mM) were mixed in the reaction medium. The free enzymes (20 U DHAK, 20 U PK_{Gstea}) or immobilized enzymes (20 U DHAK, 20 U PK_{Gstea} in 20.8 mg of biohybrid) were then added. The final volume was 12 mL. The reactions were followed by spectrophotometric assay of pyruvate, PEP, and DHAP and were completed within 45 min. The analytical yield of DHAP was 100%.

Synthesis of D-F6P

Co-immobilization of FSA_{A129S}, DHAK, PK_{Gstea}, and TPI was done as follows: a magnesium, zinc, and aluminum nitrate salt solution (4.7 mL, $\Sigma[Mg^{2+} + Zn^{2+} + Al^{3+}] = 0.1$ M, Mg/Zn/Al = 1:1:1) was added into a reactor containing DHAK (182 U, 45 mg), PK_{Gstea} (92 U, 1 mg), TPI (1638 U, 0.1 mg), and FSA_{A129S} (13 U, 2.5 mg) dissolved in Tris buffer (50 mM, pH 9.0, 15 mL). With stirring and under a nitrogen atmosphere, the pH was kept at 9.0 during the immobilization process, which was complete in 200 min. The precipitate was washed by three dispersion/centrifugation cycles with deionized water. The biohybrid (85 mg) was obtained with the following activities per mg of biohybrid: 0.14 U of FSA_{A129S}, 1.1 U of DHAK, 0.66 U of PK_{Gstea}, and 18 U of TPI. The yield of the coprecipitation was 85%. The encapsulation efficiency was 100%, and the retained activities were 50, 50, 90, and 92% for DHAK, PK_{Gstea}, TPI, and FSA_{A129S}, respectively. The biohybrid was conserved as a colloidal suspension in deionized water at 4 °C.

D-F6P was prepared by a one-pot cascade reaction by using free[17] or immobilized enzymes. Reaction mixtures were prepared with the following reagents: DHA (0.8 mmol, 2 equiv.), PEP (0.32 mmol), ATP (36 μmol), and $MgCl_2$ (10 mM). The free enzymes (20 U DHAK, 11 U PK_{Gstea}, 288 U TPI, and 3 U FSA_{A129S}) or immobilized enzymes (20 U DHAK, 11 U PK_{Gstea}, 288 U TPI, and 3 U FSA_{A129S} in 16 mg of biohybrid) were then added. The final volume was 12 mL. The reactions were followed by spectrophotometric assay of pyruvate, PEP, and D-F6P. D-F6P was isolated in 90% yield by using the co-immobilized enzymes.

Acknowledgements

This work was financially supported by the Auvergne region (Conseil regional de la region Auvergne) and the European Regional Development Fund (ERDF) through a fellowship to R.M.

Keywords: domino reactions · enzymes · immobilization · nanomaterials · phosphorylated sugars

[1] C.-J. Li, B. M. Trost, *Proc. Natl. Acad. Sci. USA* **2008**, *105*, 13197 – 13202.
[2] E. Ricca, B. Brucher, J. H. Schrittwieser, *Adv. Synth. Catal.* **2011**, *353*, 2239 – 2262.
[3] W.-D. Fessner, *New Biotechnol.* **2014**, DOI: 10.1016/j.nbt.2014.11.007.
[4] S. Schoffelen, J. C. M. van Hest, *Soft Matter* **2012**, *8*, 1736 – 1746.
[5] S. Schoffelen, J. C. M. van Hest, *Curr. Opin. Struct. Biol.* **2013**, *23*, 613 – 621.
[6] I. Oroz-Guinea, E. García-Junceda, *Curr. Opin. Chem. Biol.* **2013**, *17*, 236 – 249.
[7] J. Rocha-Martín, B. de Las Rivas, R. Muñoz, J. M. Guisán, F. López-Gallego, *ChemCatChem* **2012**, *4*, 1279 – 1288.
[8] F. Vaillant, A. Millan, P. Millan, M. Dornier, M. Decloux, M. Reynes, *Process Biochem.* **2000**, *35*, 989 – 996.
[9] Y. Ge, Y. Wang, H. Zhou, S. Wang, Y. Tong, W. Li, *J. Biotechnol.* **1999**, *67*, 33 – 40.
[10] N. Chauhan, J. Narang, C. S. Pundir, *Indian J. Med. Res.* **2014**, *139*, 603 – 609.
[11] D. Zeng, W. Luo, J. Li, H. Liu, H. Ma, Q. Huang, C. Fan, *Analyst* **2012**, *137*, 4435 – 4439.
[12] A. Salinas-Castillo, I. Pastor, R. Mallavia, C. R. Mateo, *Biosens. Bioelectron.* **2008**, *24*, 1053 – 1056.
[13] C. Forano, U. Costantino, V. Prévot, C. Taviot-Gueho in *Handbook of Clay Science* (Eds.: F. Bergaya, G. Lagaly), Elsevier Amsterdam, The Netherlands, **2013**, pp. 745 – 782.
[14] V. Prévot, C. Mousty, C. Forano, *Adv. Chem. Res.* **2013**, *17*, 35 – 83.
[15] C. Guérard-Hélaine, M. Debacker, P. Clapés, A. Szekrenyi, V. Hélaine, M. Lemaire, *Green Chem.* **2014**, *16*, 1109 – 1113.
[16] V. Hélaine, R. Mahdi, G. V. Sudhir Babu, V. de Berardinis, R. Wohlgemuth, M. Lemaire, C. Guérard-Hélaine, *Adv. Synth. Catal.* **2015**, *357*, 1703 – 1708.
[17] I. Sánchez-Moreno, V. Hélaine, N. Poupard, F. Charmantray, B. Légeret, L. Hecquet, E. García-Junceda, R. Wohlgemuth, C. Guérard-Hélaine, M. Lemaire, *Adv. Synth. Catal.* **2012**, *354*, 1725 – 1730.
[18] C. Guérard-Hélaine, B. Légeret, C. Fernandes, V. Prévot, C. Forano, M. Lemaire, *New J. Chem.* **2011**, *35*, 776 – 779.
[19] R. Mahdi, C. Guérard-Hélaine, C. Laroche, P. Michaud, V. Prevot, C. Forano, M. Lemaire, *J. Mol. Catal. B* **2015**, unpublished results.
[20] C. Mousty, O. Kaftan, V. Prevot, C. Forano, *Sens. Actuators B* **2008**, *133*, 442 – 448.
[21] I. Sánchez-Moreno, J. F. García-García, A. Bastida, E. García-Junceda, *Chem. Commun.* **2004**, *14*, 1634 – 1635.
[22] J. A. Castillo, C. Guérard-Hélaine, M. Gutiérrez, X. Garrabou, M. Sancelme, M. Schürmann, T. Inoue, V. Hélaine, F. Charmantray, T. Gefflaut, et al., *Adv. Synth. Catal.* **2010**, *352*, 1039 – 1046.
[23] M. Wang, S.-W. Huang, D. Xu, W.-J. Bao, X.-H. Xia, *Anal. Chem.* **2015**, *87*, 5831 – 5836.
[24] F. Cavani, F. Trifirò, A. Vaccari, *Catal. Today* **1991**, *11*, 173 – 301.
[25] I. Sánchez-Moreno, L. Iturrate, E. G. Doyagüez, J. A. Martínez, A. Fernández-Mayoralas, E. García-Junceda, *Adv. Synth. Catal.* **2009**, *351*, 2967 – 2975.
[26] W.-D. Fessner, D. Heyl, M. Rale, *Catal. Sci. Technol.* **2012**, *2*, 1596 – 1601.
[27] F. Camps Bres, C. Guérard-Hélaine, V. Hélaine, C. Fernandes, I. Sánchez-Moreno, M. Traikia, E. García-Junceda, M. Lemaire, *J. Mol. Catal. B* **2015**, *114*, 50 – 57.
[28] W.-D. Fessner, G. Sinerius, *Angew. Chem. Int. Ed. Engl.* **1994**, *33*, 209 – 212; *Angew. Chem.* **1994**, *106*, 217 – 220.
[29] M. D. Bednarski, E. S. Simon, N. Bischofberger, W. D. Fessner, M. J. Kim, W. Lees, T. Saito, H. Waldmann, G. M. Whitesides, *J. Am. Chem. Soc.* **1989**, *111*, 627 – 635.
[30] W.-D. Fessner, G. Sinerius, A. Schneider, M. Dreyer, G. E. Schulz, J. Badia, J. Aguilar, *Angew. Chem. Int. Ed. Engl.* **1991**, *30*, 555 – 558; *Angew. Chem.* **1991**, *103*, 596 – 599.

Received: May 30, 2015
Revised: July 1, 2015
Published online on September 1, 2015